Investigation of oxygen reduction on activated carbon electrodes in alkaline solution

Deyang Qu *

Department of Chemistry, University of Massachusetts Boston, 100 Morrissey Blvd., Boston, MA 02125-3393, United States

Abstract

Oxygen reduction has been studied on gas diffusion electrodes made from various kinds of activated carbon materials. The potentiodynamic method was used to study the electrochemical behavior of the reduction reaction, while nitrogen gas adsorption and powder X-ray diffraction were used to determine the pore size distribution and the crystal structure of the carbon material, respectively. The relationship between the catalytic activity of activated carbon and the surface content of edge orientation was discussed. The specific catalytic activity of activated carbon is determined by the percentage of the edge orientation on the surface. The higher the content of the edge plane, the lower the oxygen reduction overpotential. The reduction overpotential is also related to the effective surface area, which determines the local current density.

1. Introduction

The search for clean and renewable power sources has been a major technological and environmental activity for several decades. Among the power sources being studied are primary and secondary battery systems, and a new generation of systems based on hydrogen fuel.

Rapidly growing markets for electronic devices require primary batteries with high capacity, low self-discharge rates, good rate/pulse capacity, low cost, high reliability and most importantly, environmental friendliness. The market is currently dominated by primary MnO_2/Zn cells. The market segment is annually worth \$10 billion and is growing at a rate of 6% a year. Fuel cells have been considered as a potential candidate to reduce our dependence on fossil fuels and to diminish, or at least minimize, poisonous emissions into the atmosphere.

Oxygen reduction in alkaline electrolytes has been of great interest for decades, not only due to its known importance for alkaline fuel cells, but also due to the fact that replacing MnO_2/Zn with air/Zn chemistry in cylindrical cells is extremely appealing. The reduction of oxygen in alkaline solution has been widely investigated on various carbon materials. The 2-e reduction mechanism with the formation of hydrogen peroxide ion (HO_2^-) is widely adopted. Even though substantial disagreement remains regarding the intermediate steps during the oxygen reduction reaction in the literature [1–4], most researchers agree that adsorption of dissolved O_2 or of its one-electron reduction product, the superoxide ion $(O_2^{\cdot-})$, as well as of the intermediate hydroperoxyl radical $(HO_2^{\cdot-})$ are involved. Thus, regardless of the detailed mechanism, active sites for the adsorption of oxygen species on the carbon surface are essential for oxygen reduction.

The majority of the studies on oxygen reduction in alkaline electrolytes were on electrocatalysis by solid carbon electrodes, e.g., pyrolytic graphite [5,6], and the catalyst supported carbon electrodes [7–11]. Activated carbon and carbon black, which are the two most important materials for the gas diffusion electrodes (GDE) used in both fuel cells and air/metal cells, are hardly studied. In the limited publications on the matter, the physical properties, e.g., surface area, porosity, surface treatment and surface func-

* Fax: +1 617 287 6185.
  E-mail address: Deyang.qu@umb.edu

tionalities, have been investigated [12–16]. The close relationship between the activity of the porous carbon electrode with the surface area and the pore size distribution has been proposed: increases in specific surface area and mean pore diameter enhance the activity, and the impact of pore diameter is more profound than that of surface area [15] due to the fact that micropores may not be used for the oxygen reduction reaction [12]. An oxygen reduction reaction mechanism has been proposed [13], and oxygen gas is believed to diffuse toward the cathode surface, initially reduced on a located "active site" to yield the adsorbed superoxide ion via a reversible one-electron step. However, the nature of the so-called "active sites", which facilitate the electron transfer and possibly also provide adsorption sites for the superoxide ions, has not been reported. The present work is devoted to the investigation of the relationship between the surface structure of activated carbon and its catalytic activity for the oxygen reduction.

2. Experimental details

Ultra high surface area activated carbon materials M20 and M30 from SPECTRACORP were used as received. UMB1-5 were home-made activated carbons by modifying different pre-cursor materials through various activation procedures in order for various porosities and surface structures to be created.

Aqueous potassium hydroxide solution (30%) was used as an electrolyte in all experiments at 298 ± 2 K. All potentials reported were referred to the Hg/HgO reference electrode immersed in KOH of the same concentration as the experimental electrolyte. A Ni-mesh counter electrode was used.

A gas diffusion electrode was made with 90 wt% of activated carbon and 10 wt% of Teflon dry material. Teflon suspension (T-30) from DuPont was used. The active carbon powder was first thoroughly mixed with T-30 in a high-speed Waring blender and the paste was left to air dry. The resulting Teflon-bonded activated carbon was hot-rolled into a thin film, and then hot-pressed onto a Ni mesh current collect.

The GDE was housed in the electrochemical cell shown in Fig. 1. The activated carbon side of the GDE was forced against an O-ring by four screws in order to prevent leakage. The interfacial area between the GDE and the electrolyte was 95 mm². The Ni side of the GDE was exposed to air. A small hole was drilled on the side of the cell for the implementation of HgO/Hg reference electrode.
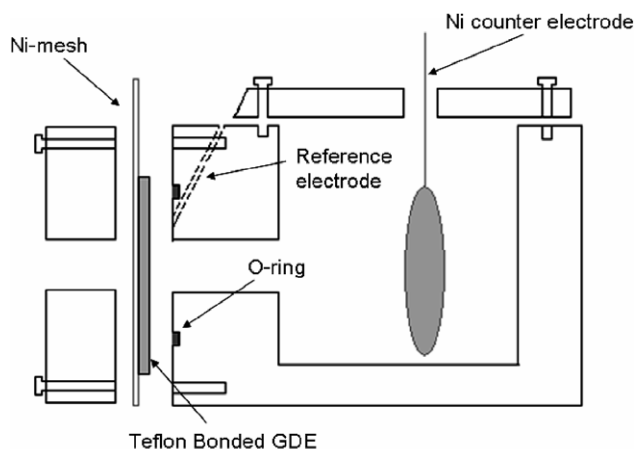

Fig. 1. Electrochemical cell used in the experiments.

Solid pyrolytic graphite rods (high order pyrolytic graphite (HOPG) and pyrolytic graphite (PG)), were sealed in the shrinkable tubing. The surface of the edge orientation was polished to a mirror finish with 3 μm polishing paper. The fresh surface of a basal orientation was revealed by placing a piece of Scotch tape in contact with the basal surface, and then peeling off a thin layer with the tape. Three pyrolytic graphite orientations were studied (basal orientation of HOPG, edge and basal orientations of PG). The basal plane of HOPG can be considered as perfect crystal, while significant amount of defects exist on the basal plane of PG. In the events where the solid graphite rods were used as the working electrodes, the electrodes were housed in a three-neck flask, and pure oxygen was bubbled through a sintered disperser for one hour before the electrochemical measurements were conducted. The interfacial area for the pyrolytic graphite electrodes was 79 mm².

An EG&G 170 potentiostat/galvanostat controlled by the Q&R Smart Date package was used for electrochemical measurements. A Micromeritics ASAP2020 porosimeter was used for the surface area and porosity measurements. Nitrogen was used as an absorbent gas. Density function theory (DFT) software from Micromeritics was also used. All X-ray powder diffraction patterns of each sample were collected using a Siemens D5000 powder diffractometer (XRD) equipped with a Cu target X-ray tube and monochrometer.

3. Results and discussion

3.1. Reduction of oxygen on the basal and edge orientation of graphite

The anisotropic electrical properties of graphite result from its crystal structure. The ratio of principal axis conductivities of single crystal graphite is higher than that of other element materials. Along the direction of the edge orientation, graphite is as conductive as a metal, while along the direction of the basal orientation, which is perpendicular to the graphene layers, it behaves like an intrinsic semiconductor. Beside the difference in electric properties, the chemical properties also differ between the two orientations. The basal plane is flat at the atomic scale and can be considered as a nearly perfect single crystal. Because there are no unsatisfied chemical bonds or free electrons, it is unlikely that functional groups will be chemically bonded to its surface, except to the defect sites with high strains. The edge plane, however, is rough and with unsatisfied valences, most of the surface functional groups would be attached on the edge plane.

A significant difference was found in the reduction of oxygen on the basal and edge orientations of graphite. Fig. 2 shows the cyclic-voltammetry profiles of the oxygen reduction on the edge layers of PG, and the basal layers of PG and HOPG, respectively. HOPG is very well crystallized graphite, its basal orientation is flat on the atomic scale and can be considered as a nearly defect free surface; the basal layer of a regular PG could have a significant amount of imperfections where the edge plane may be exposed. As shown in Fig. 2, the reduction of oxygen is inhibited on the basal plane of HOPG, and the edge orientation has the highest activity; the basal layer activity of a regular PG is in between. The results are consistent with the well-known previous reports for the oxygen reduction of pyrolytic graphite [1,5]. The catalytic activity of a graph-
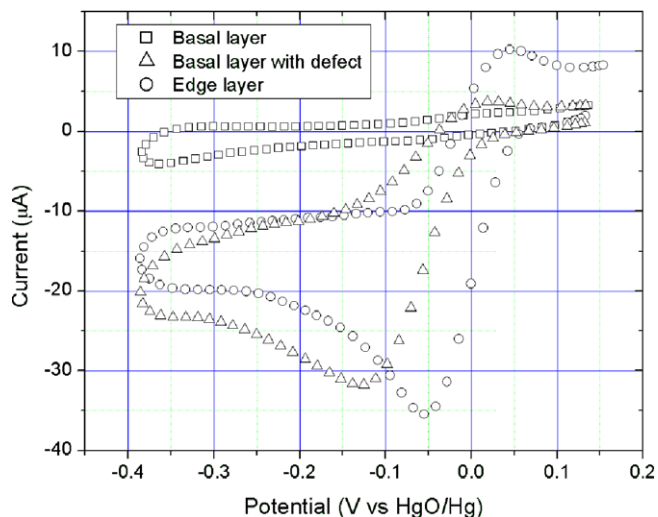
Fig. 2. Cyclic voltammetry for O_2 reduction on the surface of HOPG basal layer (marked as basal layer), PG basal layer (marked as basal layer with defects) and PG edge layer. The apparent surface area of the electrodes was 79 mm^2.

ite electrode intimately associates with the surface concentration of edge orientation.

The different behavior of the oxygen reduction on the edge and basal orientations reflects the difference in the surface electro-catalytic properties. In order for the reduction to take place, a strong interaction between the reactant and the electrode surface is required to facilitate the electron transfer and to provide the adsorption sites for the intermediates. The O_2 reduction on the basal plane should be very inhibited due to the fact that a significant fraction of the applied potential falls across the space charge region [17–19], and there are no unsatisfied valences on the basal plane to provide the sites for the adsorption of the intermediates and the functional groups. The functional groups, e.g., quinine groups may participate in the course of oxygen reduction [19].

3.2. The structure of activated carbons

Activated carbons, which are produced by either thermal activation or chemical activation, have a large surface area and a broad range of pore size distribution. Activated carbons consist of small hexagonal carbon rings, which are called "graphene sheets". Different size orientation and stacking of these sheets can be achieved by adjusting the carbon preparation method. But, in general, an activated carbon has an amorphous structure and lacks long-range three-dimensional order.

In order to graphically explain the short-range arrangement within a high surface area amorphous carbon material, Dahn et al. proposed the model of "Falling Cards" to explain the complex structure of activated carbon [20]. The "Falling Cards" model treats activated carbon as the combination of a lot of small domains that consist of a few graphene sheets in parallel. Fig. 3 shows the powder
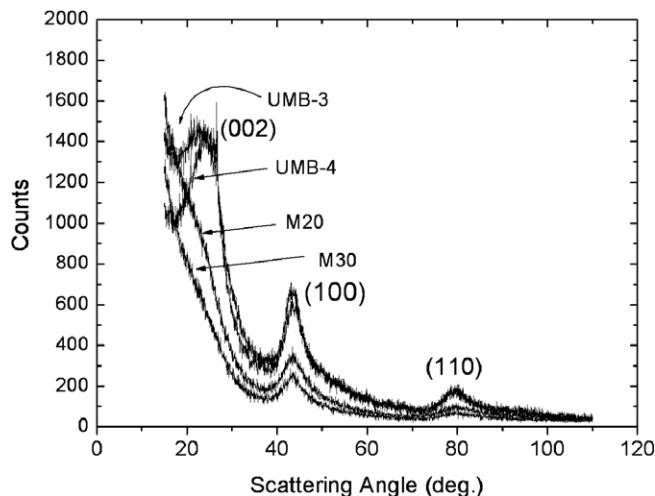

Fig. 3. Comparison of XRD profiles of activated carbon M20, M30, UMB3 and UMB4.

XRD patterns for four different activated carbons studied in this paper. The clear observation of (100) peak near 42° and (110) peak near 79° indicates that the activated carbons consist of small domains of ordered graphene sheets. In order to estimate the number of carbon sheets arranged as single layers, Liu and Dahn et al. [20] proposed an empirical parameter, R. "R" is measured as the ratio of the height of the (002) Bragg peak to the background, as illustrated in Fig. 4. It has been demonstrated by the researchers that R decreases as the single-layer content of the carbon increases. When $R = 1$, all graphene layers are randomly distributed as single layers. According to Liu's results, all activated carbon studied in this paper should contain randomly oriented single-layer and multi-layer domains. The "R" values of the activated carbon studied in this paper are tabulated in Table 1.

3.3. Oxygen reduction on the activated carbon electrodes

A GDE electrode is made with a highly porous activated carbon material. Each activated carbon has its own unique
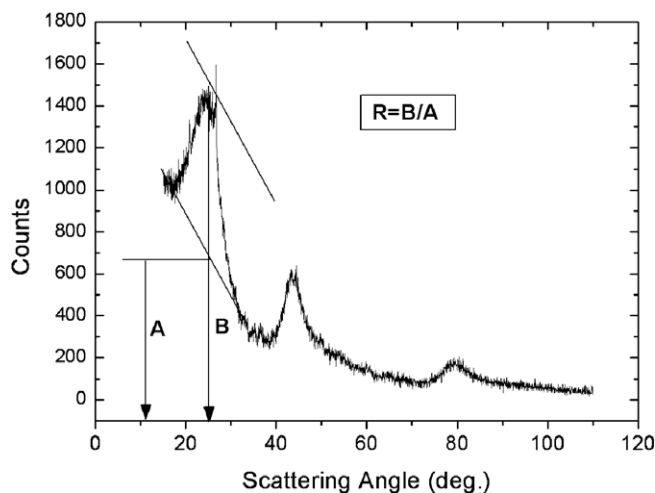

Fig. 4. The definition of the parameter R.

Table 1
Comparison of surface areas, average pore size and "*R*" value of the activated carbons

Carbon	UMB-1	UMB-2	UMB-3	UMB-4	UMB-5	M20	M30
BET surface area (m^2/g)	1198.4	787.6	1547.0	829.6	1119.3	2130.0	2571.0
DFT surface area >5 Å (m^2/g)	941.1	782.7	1210.9	717.6	904.1	1413.2	1719.0
DFT surface area >15 Å (m^2/g)	245.8	118.1	317.0	100.2	219.3	183.0	683.0
DFT surface area >50 Å (m^2/g)	40.06	64.8	22.0	16.8	44.4	6.2	37.0
Average pore size (Å)	27.3	54.6	24.6	36.9	31.9	14.7	14.95
R value	1.90	1.94	1.52	2.14	1.91	1.08	1

pore size distribution, which is engineered through the selection of pre-cursor materials and the control of activation process conditions. Fig. 5 shows the comparison of the pore size distribution of UMB2 and 4, the difference can be clearly seen. Obviously, the large pores are much easier to access by electrolyte than the small pores. The electrochemical accessibility of the pores with different sizes in the activated carbon electrode was studied by Qu using an ac impedance and transmission line model [21]. In an alkaline electrolyte, the micropores that can accommodate adsorbed nitrogen molecules at 77 K are also available for the electro-adsorption of simple hydrated ions, e.g., OH^- or K^+ at a low concentration-dependent rate in alkaline solution, thus the pores with size larger than 5 Å could be eventually accessible electrochemically [22]. However, for a GDE, not only the simple ions in the electrolyte but also dissolved oxygen molecules and solvated anion, e.g., O_2H^- have to be taken into consideration. The pores have to be large enough to accommodate the hydrated ions and Helmholtz double layers. In addition, the mobility of substances in the fine pores is more sluggish than those in the larger pores. Appleby et al. suggested that a pore diameter in the order of 18 Å would be required to facilitate an effective oxygen reduction reaction [12]. Table 1 compares the BET surface area and DFT surface areas of the pores with

sizes larger than 5 Å, 15 Å and 50 Å, respectively. It should be pointed out that BET procedures can significantly over estimate the physical surface area of micro porous materials, since the BET model of adsorption treats all adsorption sites on a surface as identically energetic, neglecting interactions among neighboring adsorbate molecules in the same layer. Instead of the phenomenological approach, it is preferable to use a molecular–based statistical thermodynamic theory that allows relating the adsorption isotherm to the microscopic properties of the system: the fluid–fluid and fluid–solid interaction energy parameters, the pore size, pore geometry, and the temperature. DFT is based on the idea that the free energy of an inhomogeneous fluid can be expressed as a functional of $\rho(r)$ and all the relevant thermodynamic functions can be calculated once the functional is known and the microscopic structure of the inhomogeneous fluid can be determined as well [23,24]. The model of slit-like pore geometry was used in the studies to extract pore size distribution information from the experimental N_2 adsorption isotherms.

Oxygen reduction proceeds principally through the peroxide pathway on carbon and graphite electrodes. The product of the 2-electron reduction is H_2O_2, which subsequently decomposes. The adsorption of superoxide $[(O_2^{\cdot -}), (HO_2^{\cdot})]$ and peroxide $[(O_2H^-), (O_2H_2)]$ may occur during the reaction [19]. Fig. 6 shows the comparison of the O_2 reduction profiles of three different activated carbon electrodes. A significant activity difference can be observed for the three electrode materials. The slope of the reduction curve in the range of high overpotential ($mA/m^2\ mV$) as shown in Fig. 6, can be used to estimate the catalytic activity of an activated carbon electrode.

The oxygen reduction overpotential of a porous activated carbon electrode is also related to the local current density (the operating current per unit true effective area). The larger the effective area, the lower the current density and the lower the overpotential of the reaction. In order to compare the catalytic activity of the activated carbon electrodes with different surface areas, specific current density is used, as plotted in Fig. 6. The surface area of the pores larger than 15 Å is assumed as an effective surface that participates in the reduction reaction.

As discussed previously, oxygen adsorption occurs preferentially on the edge planes of the carbon structure; the active sites are probably the exposed edge orientations in the matrix of an activated carbon. Thus, the catalytic activ-
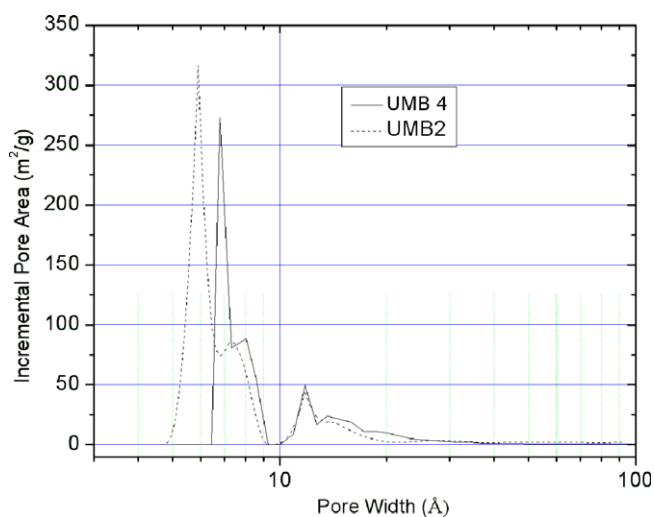

Fig. 5. Comparison of pore size distribution of activated carbon UMB2 and UMB4 calculated using DFT method from N_2 adsorption isotherm.
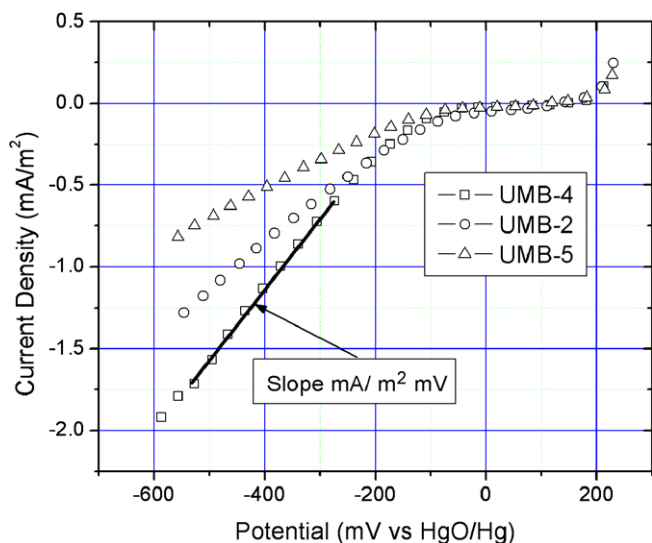
Fig. 6. Potentiodynamic for O_2 reduction at activated carbon UMB2, UMB4 and UMB5. Surface area of pores with size larger than 15 Å was used to calculate the current density.

ity of an activated carbon electrode should rely on the concentration of the edge orientation, which serves as the active site for the adsorption, facilitating the electron transfer. Fig. 7 shows the relationship of the "R" value, which stands for the concentration of a single graphene layer, with the slope of the reduction curve; representing the specific catalytic activity of an activated carbon electrode. It is clearly demonstrated that the specific catalytic activity of the activated carbon electrode is related to the surface content of the edge orientation. As "R" increases, the single-layer content decreases, and more graphene layers stack together, forming multi-layer domains with edge orientation. The specific catalytic activity of the activated carbon electrode increases as "R" increases, thus the higher the percentage of the edge orientation, the higher the intrinsic

catalytic activity for oxygen reduction. So, it could be concluded that the specific intrinsic catalytic activity of an activated carbon electrode is the function of the concentration of the edge plane exposure.

It is worth emphasizing that the overpotential of the oxygen reduction is also related to the local current density, which is proportional to the effective surface area, while the concentration of the edge orientation determines the specific intrinsic catalytic activity (per square meter). The impact of the surface area and the pore size distribution are under active investigation and will be reported elsewhere. Additionally, the electrocatalytic activity of activated carbon may also be related to the surface functional groups. For example, Sarapuu et al. [25] pointed out that the redox potential of the surface-bound quinine couple is the main factor that determines the electrocatalytic activity of the quinine-modified HOPG electrodes. The edge orientation is more preferable for the functional groups to become adsorbed than the basal orientation, thus higher concentration of the edge orientation would result of larger coverage of the functional groups.

4. Conclusions

The influence of activated carbon structure on the catalysis of oxygen reduction has been investigated. The specific catalytic activity of an activated carbon relies on the crystal orientation on its surface. The high percentage of the edge orientation results of the high catalytic activity. The edge orientation on the surface of an activated carbon serves as an "active site" for the reduction of oxygen. The difference between the edge and basal orientations may be due to the fact that O_2, superoxide and functional groups are easier to adsorb on the edge plane. The micro pores in the GDE may not be used for an oxygen reduction reaction.

References

[1] Yeager E, Krouse P, Rao KV. The kinetics of the oxygen-peroxide couple on carbon. Electrochim Acta 1964;9(8):1057–70.
[2] Appel M, Appleby AJ. A ring-disk electrode study of the reduction of oxygen on active carbon in alkaline solution. Electrochim Acta 1978;23(11):1243–6.
[3] Xu J, Huang W, McCreery RL. Isotope and surface preparation effects on alkaline dioxygen reduction at carbon electrodes. J Electroanal Chem 1996;410(2):235–42.
[4] Yang HH, McCreery RL. Elucidation of the mechanism of dioxygen reduction on metal-free carbon electrodes. J Electrochem Soc 2000;147(9):3420–8.
[5] Morcos I, Yeager E. Kinetic studies of the oxygen-peroxide couple on pyrolytic graphite. Electrochim Acta 1970;15(6):953–75.
[6] Paliteiro C. The electro reduction of oxygen on pyrolytic graphite. J Electroanal Chem 1987;233(1–2):147–59.
[7] Kao WH, Kuwana T. Electrocatalysts by electrodeposited spherical platinum micro particles dispersed in a polymeric film electrode. J Am Chem Soc 1984;106(3):473–6.
[8] Durand RR, Bencosme CS, Collman JP, Anson FC. Mechanistic aspects of the catalytic reduction of dioxygen by cofacial metalloporphyrins. J Am Chem Soc 1983;105(9):2710–8.
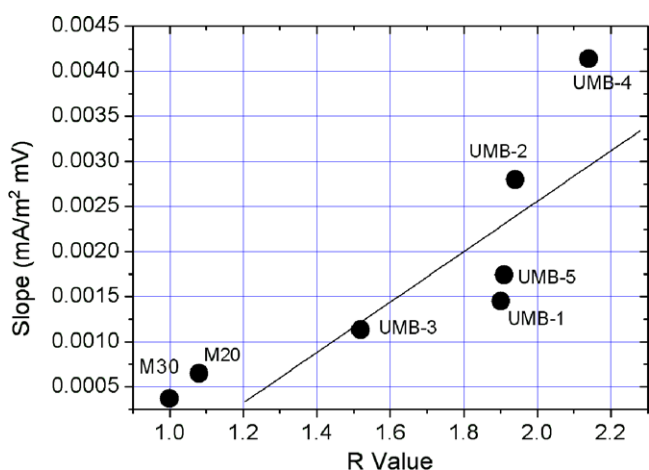
Fig. 7. Catalytic activity (the slope of potentiodynamic reduction curve as shown in Fig. 6) as a function of R value.

[9] Wang XY, Sebastian PJ, Smit MA, Yang HP, Gamboa SA. Studies on the oxygen reduction catalyst for zinc–air battery electrode. J Power Sources 2003;124(1):278–84.

[10] Lima FHB, Calegaro ML, Ticianelli EA. Investigation of the catalytic properties of manganese oxides for the oxygen reduction reaction in alkaline media. J Electroanal Chem 2006;590(2):152–60.

[11] Cao YL, Yang HX, Ai XP, Xiao LF. The mechanism of oxygen reduction on MnO_2-catalyzed air cathode in alkaline solution. J Electroanal Chem 2003;557:127–34.

[12] Appleby AJ, Marie J. kinetics of oxygen reduction on carbon materials in alkaline solution. Electrochim Acta 1979;24(2):195–202.

[13] Alcaide F, Brillas E, Cabot PL. Oxygen reduction on uncatalyzed carbon-PTFE gas diffusion cathode in alkaline medium. J Elechem Soc 2002;149(2):E64–70.

[14] Pirjamali M, Kiros Y. Effects of carbon pretreatment for oxygen reduction in alkaline electrolyte. J Power Sources 2002;109(2):446–51.

[15] Maruyama J, Sumino K, Kawaguchi M, Abe I. Influence of activated carbon pore structure on oxygen reduction at catalyst layers supported on rotating disk electrodes. Carbon 2004;42(15):3115–21.

[16] Randin JP, Yeager E. Differential capacitance study on the basal plane of stress annealed pyrolytic graphite. Electroanal Chem Interfacial Electrochem 1972;36:257–77.

[17] Qu DY. Studies of the activated carbons used in double-layer supercapacitors. J Power Sources 2002;109(2):403–11.

[18] Tarasevich MR, Sankowski A, Yeager E. Oxygen electrode. In: Conway BE, Bockris JOM, Yeager E, Khan SUM, White RE, editors. Comprehensive treatise of electrochemistry, vol. 7. New York: Plenum; 1983. p. 301–90.

[19] Yeager E. Electrocatalysts for O_2 reduction. Electrochim Acta 1984;29(11):1527–37.

[20] Liu Y, Xue JX, Zheng T, Dahn JD. Mechanism of lithium insertion in hard carbons prepared by pyrolysis epoxy resins. Carbon 1996;34(2):193–200.

[21] Qu DY. Studies of activated carbons used in double-layer capacitors. J Power Sources 1998;74(1):99–107.

[22] Soffer A, Folman N. The electrical double layer of high surface porous carbon electrode. J Electroanal Chem 1972;38(1):25–43.

[23] Webb PA, Orr C. Analytical methods in fine particle technology. Georgia: Micromeritics Instrument Corporation; 1997. pp. 53–91.

[24] Oliver JS. Modeling physical adsorption on porous and nonporous solids using density functional theory. J Porous Mat 1995;2:9–17.

[25] Sarapuu A, Helstein K, Schiffrin DJ, Tammeveski K. Kinetics of oxygen reduction on quinone-modified HOPG and BDD electrodes in alkaline solution. Electrochem Solid-State Lett 2005;8(2):E30–3.